

LETTER TO THE EDITOR

UGC 10043 in Depth: Dissecting the Polar Bulge and Subtle LSB Features

S. K. H. Bahr¹ & A. V. Mosenkov¹

Department of Physics and Astronomy, N283 ESC, Brigham Young University, Provo, UT 84602, USA

Received / Accepted

ABSTRACT

Galaxies with polar structures — of which polar-ring galaxies (PRGs) are a prominent subclass — contain components that are kinematically decoupled and highly inclined relative to the host galaxy’s major axis. Modern deep optical surveys provide a powerful means of detecting low surface brightness (LSB) features around galaxies, offering critical insights into the formation and evolution of galaxies with polar structures. UGC 10043 is an edge-on galaxy notable for its prominent bulge, which extends orthogonally to the disk plane. In addition, the galaxy displays a well-defined integral-shaped disk warp and multiple dust features crossing the bulge along the minor galaxy axis. In this work, we present new deep optical photometry of UGC 10043 down to $\mu_g = 29.5 \text{ mag arcsec}^{-2}$ and perform a detailed analysis of its LSB and polar structures. The observations reveal a stellar stream aligned along the polar axis, alongside other signatures of tidal interaction, including a flat, tilted LSB envelope that extends toward the neighboring galaxy MCG +04-37-035, with which UGC 10043 is connected by an H I bridge. Our results suggest that the polar component of UGC 10043 comprises an older, triaxial polar bulge and a younger, forming polar structure, likely originating from the ongoing disruption of a dwarf satellite galaxy, while also participating in active interaction with MCG +04-37-035.

Key words. galaxies: bulges – galaxies: evolution – galaxies: individual: UGC10043 – galaxies: peculiar – galaxies: photometry

1. Introduction

Galaxies with polar structures (PSGs) are rare and unique systems characterized by the orthogonal orientation of the major axes of the host galaxy and its polar component (Whitmore et al. 1990; Moiseev et al. 2011; Finkelman et al. 2012; Reshetnikov & Combes 2015). Several types of polar structures are known, including polar rings and disks (both inner and outer) (Bertola et al. 1999; Mosenkov et al. 2020b), polar bulges (Moiseev 2012; Reshetnikov et al. 2015), and polar halos (Crnojević et al. 2016; Mosenkov et al. 2020a; Martínez-Delgado et al. 2021).

In polar-ring galaxies (PRGs), the central host is typically an early-type galaxy that is relatively gas-poor, while the polar structure is generally a star-forming ring enriched with sub-solar metallicity gas (Spavone et al. 2010; Iodice et al. 2015; Egorov & Moiseev 2019). Polar rings are characterized by a distinct gap in the optical range, separating the polar structure from the host galaxy, whereas polar disks display a continuous distribution of material without an optical gap. Both polar rings and disks can be classified as “outer” — where the host galaxy is surrounded by a polar structure of comparable or larger size — or “inner” — where the polar structure is embedded within the larger host galaxy (see e.g. Whitmore et al. 1990; Moiseev 2012).

Polar bulges share similarities with inner polar rings and disks in that the host galaxy is larger than the polar structure. However, unlike inner polar rings/disks, polar bulges exhibit a morphology similar to normal bulges, except for their distinct tri-axial, polar orientation: as shown by Mosenkov et al. 2010; Sotnikova et al. 2012, traditional bulges in edge-on galaxies align with their stellar disks and display apparent flattening ranging from 0.3 to 0.8. Also, in comparison with the three-dimensional shape of polar bulges, inner polar rings and disks are more flat-

tened structures. Both polar bulges and inner polar rings/disks typically rotate almost orthogonally to the host galaxy disk (Moiseev 2012; Reshetnikov et al. 2015). Moreover, preexisting polar bulges can facilitate the formation of inner polar rings/disks, as observed in NGC 4698 (Corsini et al. 2012).

The morphological distinction between polar-bulge and polar-ring/disk galaxies is somewhat subjective, as it depends primarily on the relative sizes and brightnesses of their components (Reshetnikov et al. 2015). However, the same study demonstrates that polar-bulge galaxies exhibit bulge Sérsic indices and bulge-disk color differences characteristic of late-type spiral galaxies. For this study, we define polar-bulge galaxies as spiral or S0 hosts with bulges that, while typical in most respects, are distinguished by their elongation in the polar direction.

Currently, proposed formation mechanisms of PSGs include major mergers (Hibbard & Mihos 1995; Bekki 1997, 1998), minor mergers (Johnston et al. 2001; Sil’chenko et al. 2011), tidal accretion (Reshetnikov & Sotnikova 1997; Bournaud & Combes 2003), and intergalactic gas infall along cosmological filaments (Thakar & Ryden 1996, 1998; Macciò et al. 2006; Brook et al. 2008). Each of these scenarios has been confirmed by simulations and aligns with one or more observational findings (see e.g. Reshetnikov et al. 2005; Stanonik et al. 2009; Ordenes-Briceño et al. 2016; Mosenkov et al. 2022), highlighting the role of PSGs as valuable probes for studying diverse galaxy formation and evolution processes.

Deep optical surveys ($\sim 29\text{--}30 \text{ mag arcsec}^{-2}$) enable the identification and characterization of low surface brightness (LSB) polar structures that remain undetectable at the depths achieved by most standard surveys (e.g., the SDSS, which reaches a depth of $26.5 \text{ mag arcsec}^{-2}$ in the r band). By uncovering previously unknown LSB features, deep photometric

observations provide crucial insights into galactic morphology that are inaccessible with shallower data (Duc et al. 2015; Vera-Casanova et al. 2022; Martínez-Delgado et al. 2023). For instance, while the occurrence rate of PSGs was previously estimated at only 0.1% due to the limitations of existing optical surveys, recent deep imaging suggests that the true occurrence rate may be as high as 1–3% (Deg et al. 2023; Mosenkov et al. 2024).

Deep imaging has been used to expand the sample of candidate PRGs (Mosenkov et al. 2022), but similar efforts have not yet been applied to other types of polar structures, such as polar bulges. In this study, we use deep optical imaging to investigate LSB structures associated with the polar-bulge galaxy UGC 10043. Our findings demonstrate that deep imaging of PSGs can provide crucial insights into the formation mechanisms of their polar structures and, consequently, the evolutionary history of their host galaxies. Thus, deep imaging will be essential for future studies exploring the structure, formation, environment, and broader characteristics of PSGs. By treating PSGs as a coherent class of related objects rather than isolated phenomena, we can identify underlying physical patterns governing these unique systems.

UGC 10043 is an edge-on Sbc spiral galaxy located at a distance of 31.46 Mpc (Bizyaev et al. 2021). Following the prescriptions of Tully et al. (1998), Matthews & de Grijs (2004), and Springob et al. (2005), we calculate a *B*-band luminosity of $1.1 \times 10^8 L_{\odot}$ and a dynamical mass of $9.9 \times 10^{10} M_{\odot}$ for UGC 10043. It is a candidate polar-bulge system (Reshetnikov et al. 2015) and displays several distinctive features. These include a superthin disk (Bizyaev et al. 2021), a prominent major-axis dust lane that cleanly divides the galaxy into two symmetrical halves, emphasizing its pure edge-on orientation, a triaxial bulge elongated along the minor axis, and a narrow dust lane aligned with the minor axis (Matthews & de Grijs 2004; Buta 2019). Its complex morphology, coupled with the presence of a large-scale galactic wind driven by a central starburst (Aguirre et al. 2009), suggests a history involving at least one secondary event.

UGC 10043 is also a member of the small galaxy group [TSK2008] 1238 (Tully et al. 2008, 2013), where tidal interactions with the neighboring galaxy MCG +04-37-035 — confirmed by the presence of an H I bridge between the two — have likely influenced its structure (Aguirre et al. 2009). In this study, we analyze deep optical observations of UGC 10043, reaching a surface brightness limit of $29.5 \text{ mag arcsec}^{-2}$, which, for the first time, reveal a complex set of previously undetected LSB structures. These findings provide new insights into the formation of UGC 10043 and offer a broader perspective on the evolutionary pathways of galaxies with polar bulges.

This paper is organized as follows. In Section 2, we describe the data collection and reduction process for the deep photometric images. Section 3 gives a description of our image analysis. The implications of the results are discussed in Section 4, and we summarize our conclusions in Section 5.

In this article, we adopt a standard flat Λ CDM cosmology with $\Omega_m = 0.308$, $\Omega_{\Lambda} = 0.692$, and $H_0 = 67.8 \text{ km s}^{-1} \text{ Mpc}^{-1}$. Throughout this paper, all magnitudes are reported in the AB photometric system.

2. Data

Images of UGC 10043 were obtained from the DESI Legacy Survey DR10 (Dey et al. 2019) in the *g* and *r* bands, reaching pho-

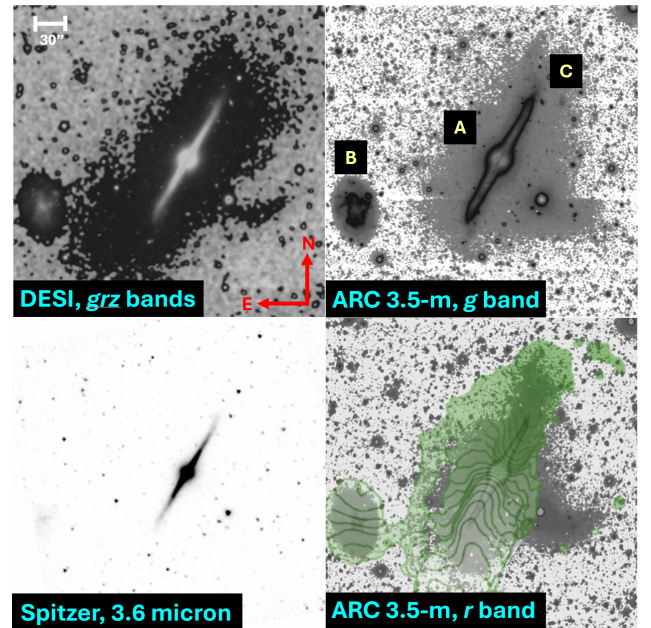


Fig. 1. Four views of UGC 10043: (clockwise from top left) the DESI Legacy Survey, the ARC 3.5-m telescope *g* and *r* bands, and the *Spitzer* Space Telescope. The ARC 3.5-m and DESI Legacy images have been enhanced to highlight the LSB stream and warp. The positions of UGC 10043, MCG +04-37-035, and MD2004 Dwarf C are indicated in the ARC 3.5-m *g*-band image by the letters A, B, and C, respectively. The Hi map from Aguirre et al. (2009) is overlaid on the ARC 3.5-m *r*-band image.

tometric depths of 29.2 and $28.5 \text{ mag arcsec}^{-2}$, respectively¹. In addition, we acquired new deep optical observations using the ARCTIC imager on the 3.5-meter ARC telescope at Apache Point Observatory, achieving depths of $29.44 \text{ mag arcsec}^{-2}$ (*g* band) and $29.38 \text{ mag arcsec}^{-2}$ (*r* band). Each filter was observed with five 15-minute exposures, yielding average PSF FWHM values of $0.67''$ in *g* and $0.75''$ in *r*. These deep optical images were primarily used to analyze LSB features in the outer regions of the galaxy.

We followed the methodology of Mosenkov et al. (2022) in preparing the deep photometric data using IMAN Python package (Mosenkov et al. 2020b), including initial data reduction (bias and dark correction, flat field correction, cosmic rays removal, astrometric correction, and photometric calibration) for the ARC 3.5-m data and rigorous masking and background subtraction for all images used.

While deep optical images are better suited for analyzing low LSB features, the inner structure of the galaxy is more effectively traced in the near-infrared, where the effects of dust extinction are significantly reduced, despite some contribution from PAH emission. This allows for a clearer view of the underlying stellar structure, particularly along the galaxy's plane and in central regions that are heavily obscured in the optical. For this purpose, we utilized an IRAC $3.6 \mu\text{m}$ image from the *Spitzer* S⁴G survey (Sheth et al. 2010), which offers a plate scale of $0.75''/\text{pixel}$ and a PSF FWHM of $1.7''$. Although the photometric depth of the IRAC image is shallower ($27 \text{ mag arcsec}^{-2}$), it is more than sufficient for modeling the stellar structure of this galaxy.

¹ Photometric depth is measured throughout this work within a $10'' \times 10''$ box at the 3σ level.

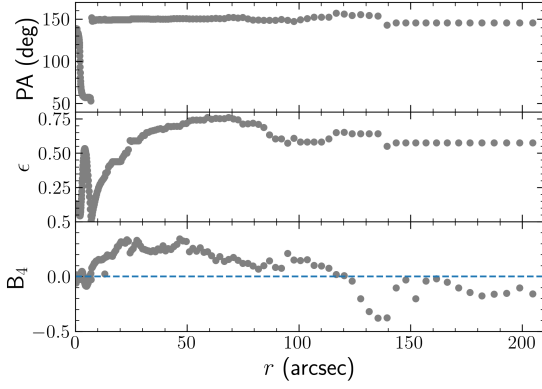


Fig. 2. Isophote fitting results: position angle, ellipticity, and B_4 for UGC 10043 as a function of distance from the center of the galaxy.

3. Results

3.1. Low-Surface Brightness Features

Both DESI and ARC deep photometry, as shown in Fig. 1, reveal a variety of low surface brightness (LSB) features surrounding UGC 10043. To quantify the galaxy’s isophotes, we performed isophote fitting using IRAF/STSDAS on the DESI Legacy grz -band image. The results, presented in Fig. 2, highlight significant variations in position angle, ellipticity, and the B_4 Fourier mode, which characterizes the shape of the isophotes (disky if $B_4 > 0$, boxy if $B_4 < 0$). In the central region, the isophotes appear approximately elliptical, with a noticeable change in isophote parameters due to the presence of the polar structure. Beyond a radius of 10", the stellar disk becomes dominant, exhibiting disky isophotes. Further out, beyond 125", the tilted thick envelope displays boxy isophotes, indicating another structural transition in the galaxy. Notably, the optical envelope is tilted by 6.5° from the plane of the galaxy, as indicated by the shift in position angle around 140" in Fig. 2, and appears to link UGC 10043 to MCG +04-37-035 (see the DESI Legacy image, Fig. 1). However, this tilt is in the opposite direction compared to both the disk warp, described below, and the gaseous envelope reported by Aguirre et al. (2009), as shown in Fig. 1. The outermost isophote of this boxy, tilted envelope has a surface brightness of $28.8 \text{ mag arcsec}^{-2}$, with a semi-major axis of 33.0 kpc and a semi-minor axis of 19.3 kpc.

The presence of an “integral sign” warp in the outer regions of the disk has been well documented in the literature. However, our deep photometry reveals that this warp has a rather irregular shape, as seen in our deep ARC images (Fig. 1). The warp angle, measured as the inclination between the galaxy plane and the line connecting the tip of the outermost isophote, is 11.4° for the northern warp and 11.3° for the southern warp at the isophote level of $31 \text{ mag arcsec}^{-2}$. The onset of the warp occurs at a distance of 7.14 kpc for the northern warp and 6.26 kpc for the southern warp.

One of the most striking LSB features of UGC 10043 is the stellar stream extending southwest of the galaxy. This stream emerges from the galactic bulge at an angle of 82.9° from the galactic plane, almost coinciding with the alignment of the polar bulge. The stream has a distinct curved shape. Following the curve of the stream in our ARC 3.5-m r -band image, we measure a total projected stream length of 10.9 kpc at the isophote level $31 \text{ mag arcsec}^{-2}$. Additionally, the stream appears to loop around the galaxy on the northeast side of the disk.

Table 1. Best fit model parameters for *Spitzer* data.

Parameter	Value
$h_{R,\text{thin}}$	1.07 ± 0.01
$z_{0,\text{thin}}$	0.08 ± 0.01
PA_{thin}	-31 (fixed)
$\mu_{e,\text{thin}}$	16.26 ± 0.03
$h_{R,\text{thick}}$	3.18 ± 0.02
$z_{0,\text{thick}}$	0.42 ± 0.01
PA_{thick}	-29.07 ± 0.02
$\mu_{e,\text{thick}}$	19.51 ± 0.02
n_{bulge}	0.40 ± 0.05
$r_{e,\text{bulge}}$	1.13 ± 0.06
$\mu_{e,\text{bulge}}$	20.83 ± 0.10
b/a_{bulge}	0.82 ± 0.04
$n_{\text{polar bulge}}$	3.79 ± 0.30
$r_{e,\text{polar bulge}}$	0.52 ± 0.03
$\mu_{e,\text{polar bulge}}$	19.36 ± 0.05
$b/a_{\text{polar bulge}}$	0.61 ± 0.02
$PA_{\text{polar bulge}}$	58.50 ± 1.25

Notes. Scale lengths h_R and scale heights z_0 (both in kpc), effective radius r_e (kpc), position angle PA (degrees), effective surface brightness μ_e (mag arcsec^{-2}), Sérsic index n , and axis ratio b/a .

3.2. Photometric Model

The photometric decomposition of UGC 10043 was performed to explore its structure and obtain the parameters of the disk and bulge, including an additional polar bulge component.

A photometric model for UGC 10043 was created using IMAN to interact with GALFIT (Peng et al. 2010). Since LSB features are not visible in the *Spitzer* image, they do not affect our decomposition. Here, we describe the creation and results of the best-fit model.

To determine the appropriate components and initial parameters for the photometric decomposition, several preliminary GALFIT runs were conducted. The finalized photometric model consists of two edge-on isothermal disks, representing the thin and thick disks, each with a truncation, as well as two Sérsic functions to account for the bulge and the polar bulge. To assess the robustness of the final model and to estimate confidence intervals for the parameter values, we performed 1000 GALFIT runs. In each run, the best-fit parameters obtained previously were used as the initial guess, and we randomly masked 10% of the pixels (bootstrapping). The fitting procedure employed the *Spitzer* PSF and the weight images provided in the S^4G database.

Table 1 reports the mean best-fit parameter values and the 1σ confidence intervals from these 1000 runs. All parameters have small errors, except for the position angle of the polar bulge, which nonetheless supports the interpretation that the secondary central component is indeed polar. The observed and model surface brightness maps, along with the residuals, are shown in Fig. 3. The model accurately reproduces the galaxy’s structure, as indicated by the green regions in the residuals.

4. Discussion

In this paper, we confirm that UGC 10043 hosts a polar bulge with an inclination angle of 89.5° relative to the galactic disk. Our decomposition of the central component into two bulge components provides further evidence of UGC 10043 being a polar-bulge galaxy. The *Spitzer* photometry reveals a flattened

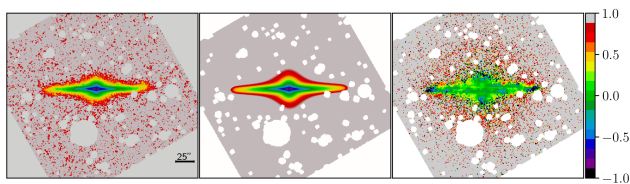


Fig. 3. Best-fit results for *Spitzer* data. Left to right: observed surface brightness, best-fit model surface brightness, relative residuals.

($b/a = 0.61$), brighter ($\mu_e = 19.36$ mag arcsec $^{-2}$) polar bulge with a relatively high Sérsic index of 3.7, characteristic of classical bulges (Fisher & Drory 2008). This polar bulge coexists with a rounder ($b/a = 0.82$), dimmer ($\mu_e = 20.83$ mag arcsec $^{-2}$) bulge with an unusually low Sérsic index of 0.4.

Matthews & de Grijs (2004) found that the bulge of UGC 10043 is triaxial, with prolate inner isophotes elongated perpendicular to the disk and outer isophotes that twist to become oblate and nearly circular. Although they did not detect compelling evidence for orthogonal rotation, the observed isophotal structure and the presence of a minor-axis dust lane suggest a component with misaligned angular momentum. This behavior is unusual for typical Sbc galaxies, but consistent with polar-bulge systems (Bertola et al. 1999; Sarzi et al. 2000; Reshetnikov et al. 2002; Corsini et al. 2003; Moiseev 2012; Reshetnikov et al. 2015). According to Gargiulo et al. (2022), a Sérsic index ≥ 2 in spiral galaxies from the IllustrisTNG50 simulation is associated with a higher fraction of ex situ stars. Thus, the Sérsic index of the polar bulge uncovered in our decomposition, combined with the morphological and tentative kinematic evidence from Matthews & de Grijs (2004), supports the interpretation of the combined bulge in UGC 10043 as a structure formed through at least one secondary event, such as tidal accretion or a minor merger.

The difference in position angle between the thin and thick disk in UGC 10043 is 1.9 ± 0.02 degrees, and the outer optical envelope is tilted by 6.5° compared to the main galaxy disk. These values are consistent with the results reported for tilted edge-on disk galaxies by Mosenkov et al. (2020b) ($5 \pm 2.3^\circ$ and $3.1 \pm 0.64^\circ$ for NGC 4452 and NGC 4469, respectively). The magnitude of the change in tilt with increasingly deep isophotes is also typical of the galaxies in Mosenkov et al. (2020b); however, the outer envelope of UGC 10043 is tilted in the opposite direction compared to the shallower isophotes.

Numerous theories have been proposed to explain the formation and prevalence of galactic warps. One widely discussed mechanism involves galaxy interactions and satellite accretion (e.g., Huang & Carlberg 1997; Kim et al. 2014; Semczuk et al. 2020). Other proposed explanations include the influence of misaligned dark matter halos (Dubinski & Kuijken 1995), discrete bending modes within a self-gravitating disk (Sparke & Casertano 1988), interactions between the gaseous disk and extragalactic magnetic fields (Battaner et al. 1990), and cosmic infall onto a disk galaxy (Shen & Sellwood 2006). However, observational evidence suggests that the most prominent warps are typically found in denser environments (e.g., Reshetnikov & Combes 1998, 1999; Schwarzkopf & Dettmar 2001; Ann & Park 2006; Ann & Bae 2016).

Observational evidence suggests that the structure of UGC 10043 has evolved through interactions with other galaxies. Located within a group environment, UGC 10043 is physically connected to its neighboring galaxy MCG +04-37-035, as shown by both H I observations (Aguirre et al. 2009) and optical

imaging (see Fig. 1). This connection indicates that MCG +04-37-035 likely contributed gas (and possibly stars) to the polar structure of UGC 10043 through tidal accretion, given the linked envelopes of the two galaxies.

Additionally, there are a possible dwarf spheroidal galaxy, MD2004 Dwarf C, located near the far edge of the disk, which may be a companion to UGC 10043, and potentially a third progenitor of the southwestern stream. However, MD2004 Dwarf C is an unlikely source of gas for either the stream or the polar bulge, as its position is within the tilted LSB envelope but not well aligned with the gas flow. Therefore, the more plausible scenario is that the gas (and possibly stellar material) originated from MCG +04-37-035. The ongoing central starburst in UGC 10043, likely fueled by tidally accreted gas, powers the galactic wind, while the star formation rate in the rest of the galaxy remains relatively low (López-Cobá et al. 2017). Furthermore, the previously detected LSB stream (Miskolczi et al. 2011), confirmed in this study, likely represents the tidal disruption of a dwarf satellite galaxy, reinforcing the evidence of a complex history of multiple interactions for UGC 10043.

5. Conclusions

From the set of polar bulge galaxies identified by Reshetnikov et al. (2015), we have selected a case study that exhibits evidence of recent or ongoing tidal interactions. The goal of this study was to investigate tidal interaction and accretion as potential mechanisms for the formation and extended lifetime of polar structures. We conducted a structural analysis of UGC 10043 using *Spitzer* 3.6 μ m data, resulting in a best-fit model that includes a thin and thick disk, a gaussian bulge, and a polar structure. Additionally, we used deep optical photometry of UGC 10043, including DESI DR10 observations and our own ARC 3.5-m imaging in the g and r wavebands, to examine LSB features surrounding the galaxy.

Our main conclusions are as follows:

- The *Spitzer* 3.6 μ m data reveals a thick disk tilted by almost 2 degrees relative to the thin disk.
- Our photometric decomposition of the *Spitzer* image also indicates the presence of both a gaussian ($n = 0.4$) bulge and a polar ($n = 3.7$) bulge (inclination angle 89.5 degrees).
- The thick disk transitions into a thick envelope with a vertical extent of 19.3 kpc, showing an even more pronounced tilt of 6.5 degrees from the thin disk for the outermost isophotes. The radius of the envelope reaches 33.0 kpc.
- Deep optical observations confirm that UGC 10043 is connected to the neighboring galaxy MCG +04-37-035, consistent with previous H I observations from Aguirre et al. (2009).
- Miskolczi et al. (2011) presented an enhanced SDSS DR7 image of UGC 10043 showing the southwestern LSB stream (see their Fig. 18) but did not discuss this feature. In our study, we confirm the presence of this stream using deeper images, demonstrating that it extends 10.9 kpc in the polar direction, with a projected inclination angle of 82.9° from the galactic plane.
- The presence of these LSB features around UGC 10043 suggests possible formation mechanisms for the polar structure and the galaxy’s pronounced disk warp, likely involving multiple accretion processes. These processes may include interactions with MCG +04-37-035 and a potential dwarf galaxy responsible for the southwestern LSB stream. Additionally, it is plausible that other distinctive characteristics of this galaxy, such as its ongoing starburst, can also be attributed to tidal accretion.

To further investigate the role of tidal interactions in the formation and evolution of diverse polar structures, it will be essential to compare these results with in-depth studies of other galaxies exhibiting various polar structure subtypes, as well as with PSGs from cosmological simulations. Future work will require deep optical observations of a large sample of PSGs to gain a comprehensive understanding of their formation mechanisms. Identifying the most common processes responsible for polar structures will provide crucial insights into how PSGs form and evolve, and how they fit within the broader hierarchical model of galaxy evolution.

Acknowledgements. We thank the anonymous referee for their helpful comments that improved this paper. Based in part on observations obtained with the Apache Point Observatory 3.5-meter telescope, which is owned and operated by the Astrophysical Research Consortium. The Legacy Surveys consist of three individual and complementary projects: the Dark Energy Camera Legacy Survey (DECaLS; NOAO Proposal ID # 2014B-0404; PIs: David Schlegel and Arjun Dey), the Beijing-Arizona Sky Survey (BASS; NOAO Proposal ID # 2015A-0801; PIs: Zhou Xu and Xiaohui Fan), and the Mayall z-band Legacy Survey (MzLS; NOAO Proposal ID # 2016A-0453; PI: Arjun Dey). DECaLS, BASS and MzLS together include data obtained, respectively, at the Blanco telescope, Cerro Tololo Inter-American Observatory, National Optical Astronomy Observatory (NOAO); the Bok telescope, Steward Observatory, University of Arizona; and the Mayall telescope, Kitt Peak National Observatory, NOAO. The Legacy Surveys project is honored to be permitted to conduct astronomical research on Iolkam Du'ag (Kitt Peak), a mountain with particular significance to the Tohono O'odham Nation. Some of the data presented in this paper were obtained from the Mikulski Archive for Space Telescopes (MAST). STScI is operated by the Association of Universities for Research in Astronomy, Inc., under NASA contract NAS5-26555. Support for MAST for non-HST data is provided by the NASA Office of Space Science via grant NNX13AC07G and by other grants and contracts. This research made use of NASA's Astrophysics Data System for bibliographic information. This research has made use of the NASA/IPAC Extragalactic Database (NED) and the NASA/IPAC Infrared Science Archive, which are funded by the National Aeronautics and Space Administration and operated by the California Institute of Technology.

References

- Aguirre, P., Uson, J. M., & Matthews, L. D. 2009, in *Revista Mexicana de Astronomía y Astrofísica Conference Series*, Vol. 35, *Revista Mexicana de Astronomía y Astrofísica Conference Series*, 201–202
- Ann, H. B. & Bae, H. J. 2016, *Journal of Korean Astronomical Society*, 49, 239
- Ann, H. B. & Park, J. C. 2006, *New A*, 11, 293
- Battaner, E., Florido, E., & Sanchez-Saavedra, M. L. 1990, *A&A*, 236, 1
- Bekki, K. 1997, *ApJ*, 490, L37
- Bekki, K. 1998, *ApJ*, 499, 635
- Bertola, F., Corsini, E. M., Beltrán, J. C. V., et al. 1999, *ApJ*, 519, L127
- Bizyaev, D., Makarov, D. I., Reshetnikov, V. P., et al. 2021, *ApJ*, 914, 104
- Bournaud, F. & Combes, F. 2003, *A&A*, 401, 817
- Brook, C. B., Governato, F., Quinn, T., et al. 2008, *ApJ*, 689, 678
- Buta, R. J. 2019, *MNRAS*, 488, 590
- Corsini, E. M., Méndez-Abreu, J., Pastorello, N., et al. 2012, *MNRAS*, 423, L79
- Corsini, E. M., Pizzella, A., Coccato, L., & Bertola, F. 2003, *A&A*, 408, 873
- Crnojević, D., Sand, D. J., Spekkens, K., et al. 2016, *ApJ*, 823, 19
- Deg, N., Palleske, R., Spekkens, K., et al. 2023, *MNRAS*, 525, 4663
- Dey, A., Schlegel, D. J., Lang, D., et al. 2019, *AJ*, 157, 168
- Dubinski, J. & Kuijken, K. 1995, *ApJ*, 442, 492
- Duc, P.-A., Cuillandre, J.-C., Karabal, E., et al. 2015, *MNRAS*, 446, 120
- Egorov, O. V. & Moiseev, A. V. 2019, *MNRAS*, 486, 4186
- Finkelman, I., Funes, J. G., & Brosch, N. 2012, *MNRAS*, 422, 2386
- Fisher, D. B. & Drory, N. 2008, *AJ*, 136, 773
- Gargiulo, I. D., Monachesi, A., Gómez, F. A., et al. 2022, *MNRAS*, 512, 2537
- Hibbard, J. E. & Mihos, J. C. 1995, *AJ*, 110, 140
- Huang, S. & Carlberg, R. G. 1997, *ApJ*, 480, 503
- Iodice, E., Coccato, L., Combes, F., et al. 2015, *A&A*, 583, A48
- Johnston, K. V., Sackett, P. D., & Bullock, J. S. 2001, *ApJ*, 557, 137
- Kim, J. H., Peirani, S., Kim, S., et al. 2014, *ApJ*, 789, 90
- López-Cobá, C., Sánchez, S. F., Moiseev, A. V., et al. 2017, *MNRAS*, 467, 4951
- Macciò, A. V., Moore, B., & Stadel, J. 2006, *ApJ*, 636, L25
- Martínez-Delgado, D., Cooper, A. P., Román, J., et al. 2023, *A&A*, 671, A141
- Martínez-Delgado, D., Román, J., Erkal, D., et al. 2021, *MNRAS*, 506, 5030
- Matthews, L. D. & de Grijs, R. 2004, *AJ*, 128, 137
- Miskolczi, A., Bomans, D. J., & Dettmar, R. J. 2011, *A&A*, 536, A66
- Moiseev, A. V. 2012, *Astrophysical Bulletin*, 67, 147
- Moiseev, A. V., Smirnova, K. I., Smirnova, A. A., & Reshetnikov, V. P. 2011, *MNRAS*, 418, 244
- Mosenkov, A., Rich, R. M., Koch, A., et al. 2020a, *MNRAS*, 494, 1751
- Mosenkov, A. V., Bahr, S. K. H., Reshetnikov, V. P., Shakespear, Z., & Smirnov, D. V. 2024, *A&A*, 681, L15
- Mosenkov, A. V., Reshetnikov, V. P., Skryabina, M. N., & Shakespear, Z. 2022, *Research in Astronomy and Astrophysics*, 22, 115003
- Mosenkov, A. V., Smirnov, A. A., Sil'chenko, O. K., et al. 2020b, *MNRAS*, 497, 2039
- Mosenkov, A. V., Sotnikova, N. Y., & Reshetnikov, V. P. 2010, *MNRAS*, 401, 559
- Ordones-Briceño, Y., Georgiev, I. Y., Puzia, T. H., Goudfrooij, P., & Arnaboldi, M. 2016, *A&A*, 585, A156
- Peng, C. Y., Ho, L. C., Impey, C. D., & Rix, H.-W. 2010, *AJ*, 139, 2097
- Reshetnikov, V., Bournaud, F., Combes, F., et al. 2005, *A&A*, 431, 503
- Reshetnikov, V. & Combes, F. 1998, *A&A*, 337, 9
- Reshetnikov, V. & Combes, F. 1999, *A&AS*, 138, 101
- Reshetnikov, V. & Combes, F. 2015, *MNRAS*, 447, 2287
- Reshetnikov, V. & Sotnikova, N. 1997, *A&A*, 325, 933
- Reshetnikov, V. P., Faúndez-Abans, M., & de Oliveira-Abans, M. 2002, *A&A*, 383, 390
- Reshetnikov, V. P., Savchenko, S. S., Mosenkov, A. V., Sotnikova, N. Y., & Bizyaev, D. V. 2015, *Astronomy Letters*, 41, 748
- Sarzi, M., Corsini, E. M., Pizzella, A., et al. 2000, *A&A*, 360, 439
- Schwarzkopf, U. & Dettmar, R. J. 2001, *A&A*, 373, 402
- Semczuk, M., Łokas, E. L., D'Onghia, E., et al. 2020, *MNRAS*, 498, 3535
- Shen, J. & Sellwood, J. A. 2006, *MNRAS*, 370, 2
- Sheth, K., Regan, M., Hinz, J. L., et al. 2010, *PASP*, 122, 1397
- Sil'chenko, O. K., Chilingarian, I. V., Sotnikova, N. Y., & Afanasiev, V. L. 2011, *MNRAS*, 414, 3645
- Sotnikova, N. Y., Reshetnikov, V. P., & Mosenkov, A. V. 2012, *Astronomical and Astrophysical Transactions*, 27, 325
- Sparke, L. S. & Casertano, S. 1988, *MNRAS*, 234, 873
- Spavone, M., Iodice, E., Arnaboldi, M., et al. 2010, *ApJ*, 714, 1081
- Springob, C. M., Haynes, M. P., Giovanelli, R., & Kent, B. R. 2005, *ApJS*, 160, 149
- Stanonik, K., Platen, E., Aragón-Calvo, M. A., et al. 2009, *ApJ*, 696, L6
- Thakar, A. R. & Ryden, B. S. 1996, *ApJ*, 461, 55
- Thakar, A. R. & Ryden, B. S. 1998, *ApJ*, 506, 93
- Tully, R. B., Courtois, H. M., Dolphin, A. E., et al. 2013, *AJ*, 146, 86
- Tully, R. B., Pierce, M. J., Huang, J.-S., et al. 1998, *AJ*, 115, 2264
- Tully, R. B., Shaya, E. J., Karachentsev, I. D., et al. 2008, *ApJ*, 676, 184
- Vera-Casanova, A., Gómez, F. A., Monachesi, A., et al. 2022, *MNRAS*, 514, 4898
- Whitmore, B. C., Lucas, R. A., McElroy, D. B., et al. 1990, *AJ*, 100, 1489